Wireless Pers Commun (2017) 95:5039–5056
DOI 10.1007/s11277-017-4144-0

Antennas and Channel Characteristics for Wireless Networks on Chips

William Rayess[1] · David W. Matolak[1] · Savas Kaya[2] · Avinash Karanth Kodi[2]

Published online: 19 April 2017
© Springer Science+Business Media New York 2017

Abstract We review the current state of the art on antennas for use in wireless networks on chips (WiNoCs) and also provide results on wireless channel characteristics in the WiNoC setting—the latter are largely absent from the literature. We first describe the motivation for constructing these miniature networks, aimed at improving efficiency of future multi-processor integrated circuits. We then discuss the implications for antennas: in addition to the usual antenna parameters for communication links (gain, impedance match, pattern), this includes important structural and multiple-access considerations. After a review of the literature and a summary of published antenna characteristics and future challenges, we present example results for a representative structure to illustrate antenna performance and WiNoC channel characteristics.

Keywords Wireless network on chips · Multi-processor integrated circuits · Delay spread · Insertion loss · Zero forcing equalization · Decision feedback equalization · Antenna characteristics · HFSS

✉ William Rayess
rayess@email.sc.edu

David W. Matolak
matolak@sc.edu

Savas Kaya
kaya@ohio.edu

Avinash Karanth Kodi
kodi@ohio.edu

[1] Department of Electrical Engineering, University of South Carolina, Columbia, SC 29208, USA

[2] School of Electrical Engineering and Computer Science, Ohio University, Athens, OH 45701, USA

1 Introduction

Future integrated circuits (ICs) will contain many processing cores—hundreds to thousands—and these types of ICs are often termed chip multiprocessors (CMPs) [1]. Present CMPs employ exclusively wired links for transferring data between cores. As the number of cores grows, wire dimensions must become smaller, creating larger resistances and consequently increasing required transmit power levels [2]. Routing of wires between many cores also consumes valuable chip area, and for communication between cores that are relatively far apart on the IC, multiple links (hops) must be used, which increases the communication latency.

To alleviate these problems, wireless networks on chips (WiNoCs) are being investigated [3–6]. Such WiNoC CMP interconnect networks will have dimensions on the order of a few cm ("attocells"), and will require data rates on the order of 10 Gbps per link between cores to be competitive with wired links. It is likely that WiNoCs will *complement* wired links, and not completely replace them. Such small wireless networks present many engineering challenges, since in addition to the large required data rates, WiNoCs must also minimize power consumption. Hence devices employed in the transceiver circuits must be both power efficient and compact. To be most effective, WiNoCs must also provide communication links between multiple pairs of cores, and ideally such connectivity should be adaptable according to inter-core traffic (connectivity) demands. Thus effective multiple access schemes must be employed to share the limited radio spectrum spanned by WiNoC transceiver devices.

In [2] we provided an overview of WiNoC engineering challenges. With many cores requiring large inter-core data rates, the amount of radio spectrum required for WiNoCs will be large (tens of GHz or more), and this means that carrier frequencies must be at tens of GHz and higher, possibly into the terahertz or optical range. At such frequencies, in addition to challenges in designing transceiver circuitry (e.g., oscillators, amplifiers, filters, etc.), the design and fabrication of effective antennas is also critical for WiNoC success. The antennas are an integral part of the wireless channel, which presents its own challenges in this unique environment. In this paper we discuss the antenna design problem, review the options thus far explored in the literature, and provide some example results for WiNoC antenna designs and wireless channels for WiNoC links.

The remainder of this paper is organized as follows: Sect. 2 describes the overall WiNoC antenna design problem, the physical WiNoC environment in which the antennas will operate, and the primary antenna characteristics of interest for WiNoC applications, along with a description of channel characteristics?. In Sect. 3 we review the literature on WiNoC antennas, classify the various antenna types, and provide representative values for key antenna parameters.[1] Section 4 provides examples of WiNoC antenna designs and corresponding channel characteristics, and in Sect. 5 we conclude.

2 WiNoC Antenna and Channel Characteristics

Generally speaking, the antenna is a transducer that at the transmit end converts the guided signal it accepts from a transmission line or source to a radiated signal propagating through a (mostly "unguiding") medium. The receiving antenna performs the inverse transduction.

[1] Since virtually nothing has appeared in the literature on practical WiNoC channel characteristics, we do not have an explicit literature review for this area; selected relevant references on this are cited throughout.

The effectiveness of these transductions quantifies the antenna's efficiency, which is one important parameter for the WiNoC communication link. A second important parameter is the antenna's bandwidth—how wide a spectrum it can pass without appreciable distortion, while maintaining its efficiency and gain. For WiNoCs, if the antenna cannot support signals of bandwidths on the order of 5–10 GHz (for data rates at or above 5–10 Gbps), multiple frequency-band-specific antennas will be required for transmission and reception. Another important antenna parameter is the antenna's gain, which measures how effectively the antenna radiates in one (desired) direction over other directions. Finally, for WiNoCs, the antenna's actual physical size is important, as several antennas must fit within the IC. In this section we discuss these issues in the context of WiNoCs.

2.1 Structural Configurations

Since the attocell WiNoC must fit with*in* an IC, the antenna's physical characteristics are important considerations in a feasible design. Conventional wire antennas are often vertically oriented, which in the WiNoC realm would mean "growing" such wires out of or on top of a substrate. With strict limits on heights (perhaps a few tenths of a mm), for such antennas to be on the order of one-quarter wavelength ($\lambda/4$), they must operate at frequencies of 300 GHz and above within air (or a vacuum). For the same wire length, antenna resonant frequencies would decrease proportionally to the dielectric refractive index if the antenna and wireless link are embedded within a dielectric. Horizontally-oriented wires could be slightly larger, but still need to be small enough to fit many antennas within the WiNoC. Horizontal wires may be more easily fabricated as printed antennas, and these can be generalized to a number of planar structures such as patches, meander or folded dipoles, etc. In fact, such planar structures dominate the literature (as discussed in the next section), even though in general they radiate broadside, i.e., up and away from the substrate, instead of along the substrate toward a corresponding receiver antenna.

Aperture antennas are desirable from the perspective of their high gain and small beamwidth, which can aid in the spatial isolation of co-channel signals propagating across the WiNoC. Their disadvantage is that they must generally be electrically large (many λ) to attain high gain and small beamwidth. Producing aperture structures to radiate and receive across the WiNoC is not a simple fabrication problem, although some basic structures (e.g., corner reflectors) may be possible in some cases. The electrically-large size requirement also implies very high frequencies (again, hundreds of GHz) to ensure these structures occupy minimal WiNoC chip area. Operating at frequencies of hundreds of GHz also provides the ample bandwidth required for the WiNoC.

Such structural considerations are relaxed when the antennas and the environment through which they radiate and receive is separated from the rest of the WiNoC components. This can be attained using vias in multi-layer substrates, for example, in which all WiNoC transceiver components are on a layer (or layers) below the (top) layer that contains antennas and the propagation medium, covered by the IC casing or packaging. As long as the vias can yield a good impedance match to the antenna, the antenna layer can be designed largely "on its own," allowing more options to attain good performance with the transmitter and receiver antennas across the confined wireless channel.

Figure 1, from [7], illustrates a *conceptual* WiNoC, where in (c) is shown the overall 16-core "landscape," with printed L-shaped antennas to the upper right of each core; part (b) shows a closer view of a core and its wireless transceiver sections, and part (a) shows an electron microscope photograph of multiple metallization layers in a Pentium 4 processor.

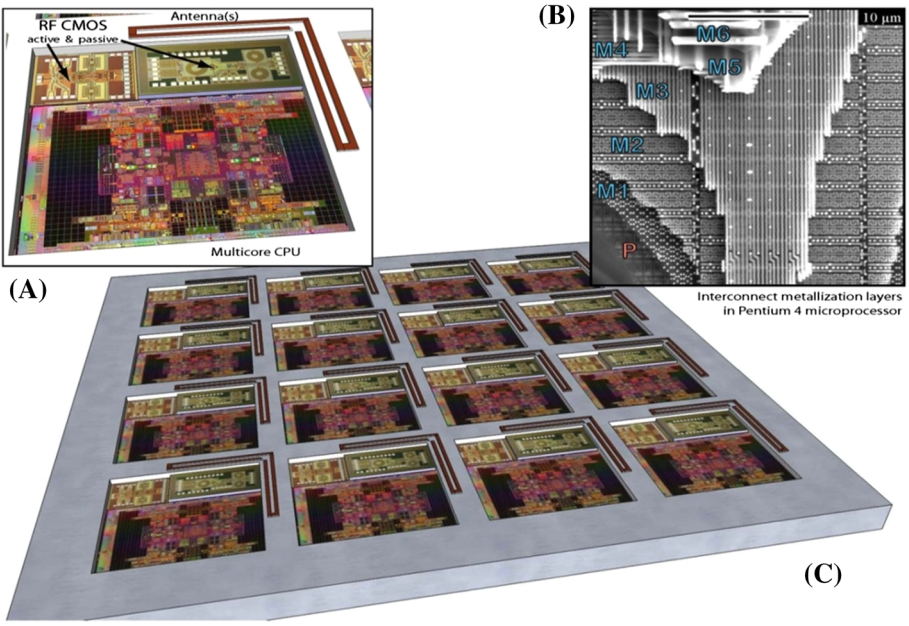

Fig. 1 Conceptual illustration of a WiNoC landscape: **a** close up of one cluster of cores along with RF transceiver components and L-shaped antenna; **b** actual electron microscope image showing multiple metallization layers used for interconnections in a single-core Pentium 4® microprocessor by Intel (*scale bar* is 10 μm); and **c** global layout of 16-cluster IC design. (From [2], used with permission.)

The layer denoted "M6" is atop all these metal layers, and could constitute the layer where the WiNoC antennas reside.

2.2 Multiple Access Considerations

In typical communication systems for terrestrial applications, data rates are low enough so that a single antenna is often sufficient for operation at one of many frequencies within a designated frequency band, or several bands that are close in frequency. In some applications such as cellular phones, when multiple frequency bands must be supported, separate antennas are used for the different bands; such multi-band structures must still be small in a relative sense, and this is sometimes attained by clever use of part of the antenna structure for one band, and use of the entire structure for another.

For the WiNoC case, data rates in excess of 10 Gbps imply bandwidths of 10 GHz or more, at least initially when binary modulation schemes are most likely because of their simplicity and energy efficiency. When multiple signals are transmitted across the WiNoC in a frequency division arrangement, either wideband antennas or multiple antennas tuned to different bands will be needed. Wideband antennas have the disadvantage that they too are often electrically large (although as we will show with our design, a properly designed monopole can attain a fairly large bandwidth). Using multiple antennas to span the very wide WiNoC spectrum is a logical choice, but this requires additional care in ensuring that the antennas are still compact and mutual coupling effects are minimized. The use of multiple antennas will also complicate and increase the size of impedance matching and antenna feed networks. A possible advantage to the use of limited-bandwidth antennas is a

relaxation on filtering requirements within the transceiver, since the antenna itself provides some of the filtering function.

If any spatial adaptation is attempted, this could require rapid changes to antenna feed amplitudes and phases, which means rapid adjustment of tuning element values. For most discrete components, this should be achievable, but adjustment precision and range vary considerably across technologies (see [2]), so initial WiNoCs may need the "buffers" of guard bands and guard times to ensure minimal cross-transceiver interference.

Finally here, unless very strong filtering can be used in both transmitters and receivers, when transmitter and receiver are in close proximity, the high power transmissions will interfere with reception of low level signals. This is the well-known "co-site" problem. To ameliorate this problem, transmit and receive bands should be separated in frequency as much as possible and for transmission and reception in different directions, the antennas should have very good spatial isolation.

2.3 Overview of WiNoC Channel Characteristics

We reported on WiNoC channel characteristics in [7], but here provide a brief summary of this area for completeness, and to serve as an introduction to the channel results we describe in Sect. 4. When addressing channel modeling, it is crucial to specify the physical landscape of the environment—in our case the WiNoC. Such landscape specification consists of the physical dimensions of the WiNoC in addition to the electrical properties, such as conductivity, permittivity, and permeability, of all objects and layers through which electromagnetic waves propagate and interact with as they travel between a transmitter and a receiver.

In Fig. 2, we define the landscape with all the materials and dimensions. Note that with the presence of metallic reflectors, a dielectric slab, and a ceramic cover, accurate deterministic channel modeling would be very challenging, and thus we employ simulations in

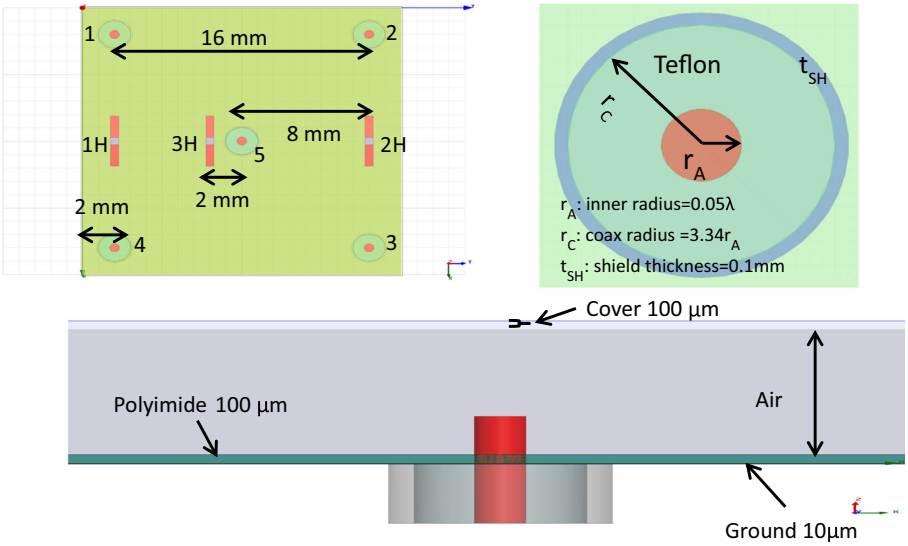

Fig. 2 Simulation model. *Bottom left* cross-section; *upper left top view* showing monopoles near corners of chip; and, *upper right* close-up *top view* of quarter wave monopole

HFSS to analyze the channel. This analysis yields attenuation and dispersion characteristics over frequency bands of interest, over certain link distances. The antennas are inherently included in our models.

The WiNoC channel is time-invariant since both transmitter and the receiver are fixed. However, multi path components will be present mainly due to the conducting surfaces present in the landscape and this will result in dispersive channels. Even small amounts of dispersion—on the order of few picoseconds—will be performance limiting since we are aiming for tens of gigabits per second data rates. We provide specific dispersion values for different channels in terms of root mean square delay spread.

3 Related Work on Antennas

We have divided this antenna review into two categories: intra-chip antennas and inter-chip antennas. The first category is directly applicable to WiNoCs, and the second may be suitable if antennas are modified (reduced in size). Table 1 contains a summary of the results from the literature review.

3.1 Intra-chip Antennas

As a result of rapidly expanding applications for sensor networks, RFID tags and system-on-chip integration, intra-chip antennas have recently drawn attention. In [8], the authors analyzed several antenna structures and produced simulation results for transmission gain at microwave frequencies. Although these frequencies are too low for most WiNoC applications, we provide results for completeness. The transmission gain is the decibel sum of transmit and receive antenna gains plus the path gain; when measured it is essentially the scattering parameter S_{21}, which quantifies gain from port one to port two. As expected, meander, zigzag, and folded structures showed higher gains than linear dipoles (all structures are planar, printed on substrate material). It is difficult to separate with precision the actual antenna gains and channel attenuations from these transmission gain values, since this requires an assumption for the path gain (or loss). Thus our antenna gain estimates cited throughout are of limited accuracy, since we employ only the very simplest of path loss models, but the *relative* gain values among the different antenna types is accurate. The transmission gain for the linear dipole pair in [8] was between approximately -70 to -50 dB for the frequency range 1–8 GHz with maximum gain occurring near 6 GHz. The meander dipole had a gain between 10 and 15 dB larger, with the peak value occurring at around 5.8 GHz, and the folded dipole had a gain between 0 and 25 dB larger than the dipole, with its peak value occurring near 6.5 GHz. If we employ the free space loss model, the transmission gains cited would yield maximum antenna gains of approximately -16.9, -13.9, and -24.3 dB for the meander, folded dipole, and linear dipole, respectively. The size of these antennas ranged from 8 to 9 mm and the link distance was 4.7 mm, hence far-field conditions are not attained for our (absolute) antenna gain estimates. The simulations in [8] were done using Sonnet® Suites™.

In [9], the authors investigated the effect on the transmission properties of an on-chip dipole antenna when a diamond layer was inserted between a silicon substrate and its heat sink. The size of the antenna simulated in HFSS was 2 mm. The range of simulation frequencies was 5–40 GHz. The transmission gain of the on-chip dipole antennas was estimated for different link distances. It was concluded that a higher gain could be achieved

Table 1 Summary of WiNoC antenna characteristics from the literature

References	Antenna size	Bandwidth B frequency range Δf	Antenna gain (dB)	Impedance (Ω)	Efficiency	Comments
[8]	8.9 mm	$\Delta f = 1.8$ GHz	−16.9, −13.9, 24.3	N/A	N/A	Gains: meander, folded dipole, linear dipole, respectively Gains estimated from free-space (not in far field) Simulation results (Sonnet)
[9]	2 mm	$\Delta f = 5$–40 GHz	−7.9, −2.9	~75	N/A	Gain estimated from free-space for 10 Ω-cm, 100 Ω-cm substrates, respectively, each w/0.35 mm diamond layer beneath (not in far field)
[10]	2.9 mm	$\Delta f = 1$–12.4 GHz (VNA) $\Delta f = 1$–20 GHz (HFSS)	−27 to−21 (measured) −14 to −22 (simulated)	N/A	3–6%	Bandwidth ~ frequency range in which $S_{11} < -10$ dB Multiple designs yielded several smaller frequency ranges, bandwidth up to 11.4 GHz Gain estimated from free-space (not in far field)
[11]	2 mm	$\Delta f = 6$–18 GHz	−19 (meander)	~150	N/A	Bandwidth not quantified in terms of S_{11} or S_{21} Gain estimated from free-space (not in far field)
[12]	0.45 mm	$B_1 = 14$ GHz $B_2 = 7$ GHz	−8 (inverted F) −14 (dipole)	50	9% (inverted-F) 2% (dipole)	Bandwidth ~ frequency range in which $S_{11} < -10$ dB Inverted-F ~ 51–65 GHz; dipole ~ 58–65 GHz
[13]	1 mm × 1 mm	$B = 120$ GHz (0.6–0.95 THz)	8.25 at 852 GHz	Matched with feed	88.3% at 852 GHz	Bandwidth ~ frequency range in which $S_{11} < -10$ dB Resonates at 693.45, 797.4, and 852 GHz Size is 2D since patch antenna
[17]	4 mm	$B = 8.5$ GHz (dipole pair) $B = 25$ GHz (phased array)	−11.51 (phased array) −21.6 (aligned dipole pair) −32.2 (opp. dipole pair)	N/A	N/A	Bandwidth ~ frequency range in which $S_{11} < -10$ dB Dipole pair 14.5–23 GHz, resonating at ~16 GHz, phased array resonating at ~22 GHz λ/2 dipole length 4 mm; array of four λ/4 monopoles arranged in square of side length 2 mm All gains at 20 GHz

Table 1 continued

References	Antenna size	Bandwidth B frequency range Δf	Antenna gain (dB)	Impedance (Ω)	Efficiency	Comments
[18]	0.3 mm	$B_{3dB} = 16$ GHz	3.9	N/A	N/A	Center frequency 62.5 GHz 16 GHz 3 dB bandwidth from S_{21}
[19]	1.4 × 0.9 mm	$B_{3dB} = 72$–120 GHz (48 GHz)	−1.5	N/A	N/A	Bandwidth is 3 dB gain bandwidth; peak at 90 GHz
	1.2 × 0.6 mm	$B = 5$ GHz, $B_{3dB} = 20$ GHz	−1.4	50	N/A	Bandwidth ~ frequency range in which $S_{11} < -10$ dB, resonating at 140 GHz; $B_{3dB} = 136$–156 GHz
	0.6 × 2 mm	$B_{3dB} = 3$ GHz	−1	50	N/A	Peak gain at 140 GHz
	0.7 × 0.7 mm	$B = 10$ GHz	−2	50	N/A	Bandwidth ~ frequency range in which $S_{11} < -10$ dB, from 138 to 148 GHz, and resonating at 141 and 146 GHz
[20]	2 × 2.3 mm	$B = 50$–85 GHz for horizontal case, $B = 60$–65 GHz and $B = 75$–85 GHz for vertical case	−3 ("H" & 60 GHz) 3.5 ("V" & 60 GHz) −2.1 ("H" & 77 GHz) 4.8 ("V" & 77 GHz)	N/A	N/A	Bandwidth ~ frequency range in which $S_{11} < -10$ dB "H" denotes horizontal position and "V" vertical polarization

with a diamond layer (0.35 mm thick) atop the substrate than without the layer. Transmission gain was largest from 15 to 40 GHz with the 0.35 mm thick diamond layer; link distance was less than 3 mm. The corresponding antenna gain, assuming a free space model, with the lower resistivity silicon substrate (10 Ω-cm) would be −7.9 dB. With a higher resistivity substrate (100 Ω-cm), the corresponding antenna gain would be −2.9 dB. A complication here again is that the link distance of 1 mm is *not* in the far field at 26 GHz—nonetheless, the relative antenna gain between the cases is accurate. Additional impedance matching networks are needed in the configuration in [4] since throughout the simulation, the resistances were above 50 Ω. In addition, adding a diamond layer would increase the overall chip implementation cost and complexity.

The authors in Ref. [10] investigated meander antennas with different pitches, lengths, widths, and numbers of turns. These antennas are printed conductors that resemble "square wave" shapes fabricated on a P-type SiO_2 substrate. HFSS was used to conduct simulations. The authors found that increasing the pitch length and number of turns while decreasing the antenna width did increase the radiation efficiency. Table 1 has additional specifications.

In a very early paper in the field, the authors of [11] investigated short linear, meander, and zigzag dipole antennas experimentally. These antennas were formed on a silicon wafer. Table 1 summarizes results. In [12], two kinds of antennas were realized, the inverted-F and dipole. Their characteristics were also investigated via simulations (HFSS) and are shown in Table 1.

In [13], the author investigated the effect of using metamaterial crystal substrate with*in* the dielectric layer on which a rectangular microstrip patch antenna was mounted. This reference employs simulations (CST Microwave Studio) to determine antenna characteristics (Table 1) for operation at THz frequencies. For interested readers, references [14–16] report on designs in the high mm-wave and sub-THz frequency ranges.

The authors of [17] compared the performance of a dipole antenna pair with a phased array pair for on-chip communication. The array consisted of four orthogonal quarter wave monopole linear arms that are fed differentially. Their simulations were done using CST Microwave Studio, with results again in Table 1.

Ref. [18] described a WiNoC in which printed zig-zag antennas are used. The authors discussed at length the required connectivity and routing, but also described the main antenna features. Antenna gains were approximately −18.5 dB with a center frequency near 63 GHz.

Ref. [19] presented four designs for on chip antennas operating at 90 and 140 GHz, and compared their performance; see Table 1. The antennas were a bowtie-shaped slot antenna, a cavity-backed slot antenna, an extremely flat waveguide slot antenna, and an E-shaped patch antenna.

The authors of [20] designed, fabricated and measured the performance of a dual band Buckled Cantilever Plate triangular fractal antenna on flexible polyamide at 60 and 77 GHz. The movable plate enables horizontal and vertical polarization on the same chip. An increase of 6 dB in gain was observed in the vertical position compared to the horizontal.

3.2 Inter Chip Antennas

Due to the availability of unlicensed bands in the 60–90 GHz range for several upcoming applications such as vehicular radars and in-room multimedia links, as well as commercially available RF-CMOS processes in the mm-wave regime, inter-chip antennas are also

relevant for the WiNoC problem. For instance, Ref. [21] reported on results using an ultra wide band triple "twiggy" antenna that was developed using 65 nm CMOS technology. No explicit antenna parameters were provided.

In [22] the authors proposed the design of a two-antenna array at 60 GHz for chip-to-chip communication, with simulations done using HFSS. Despite the fact that the array antenna offers an increase in gain of 5 dB in the horizontal direction over a single antenna, a crucial characteristic not reported in [22] is the physical size of these antennas. A similar design in [23] consists of a four-element array that achieves 8 dB increase in gain over the single antenna in the diagonal direction with a 30 GHz bandwidth at 60 GHz.

In [24], a dielectric waveguide with a high dielectric constant was used under a silicon chip to improve the efficiency and transmission gain of the on-chip antenna. Efficiency and gains were investigated as functions of the silicon resistivity and thickness. The gain increased with a thinner silicon substrate. Efficiency and transmission gain improvements of 50% and 25 dB, respectively, were seen at a transmission distance of 20 mm with the thinner substrate. Thus the paper notes an important fabrication point that large relative permittivity dielectrics found in sub-45 nm MOSFET gate stacks may also be used as the top insulator/passivation layers before the antennas are fabricated.

Ref. [25] presents results for different patch antennas that were designed with various gap configurations; simulated values of return loss were provided. Two of the five types of patch antennas with different gap configurations were fabricated, and the experimental results showed a difference of 1.5 GHz in the resonant frequency between measurements and simulations. A worst case transmission gain of −47 dB for a chip-to-chip link of distance 35 mm yields an estimate of approximately −3.75 dB for the antenna gain (again assuming free space).

The authors of [26] designed a wireless inter-chip link using bond-wire antennas. The chip was fabricated using 180 nm SiGe technology. Data rates of 2–6 Gbps were achieved over distances from 0.5 to 4 cm, at a center frequency of 43 GHz. Antenna gains were measured to be approximately −1.4 dB.

In [27], the authors reviewed the use of on-chip antennas for over the air communication and presented ways to increase communication range. To achieve this, the authors suggest using 6 mm monopole antennas operating at 5.8 GHz instead of 3 mm dipole antennas operating at 24 GHz in addition to thinning the silicon substrate below the antennas from 670 to 100 μm. Note that decreasing the operating frequency increases range naturally, but also generally has the undesirable effect of reducing bandwidth. The antenna gains are highly dependent on their height from the ground plane; for example, gains drop by 20 dB when the height decreases from 52 to 5 mm. With the original ("unthinned") substrate, the antenna gains are approximately −12 dB whereas in the thinner substrate case, the on-chip 24 GHz dipole and 5.8 GHz monopole gains are −7 and −11 dB, respectively. Interested readers who would like more insight on this topic are referred to [28].

3.3 Additional Remarks

From Table 1, we can draw several conclusions regarding WiNoC antenna design:

1. research to date has been focused on microwave and low-millimeter wave frequencies, which is likely not high enough to support future WiNoC data rates.
2. most antenna gains found in the literature, except for [13, 18, 22, 23] are less than 0 dB, which means that the antenna adds *losses* to the transmission.

3. printed antenna structures are most common, with non-monotonic effects versus frequency for substrate thickness.
4. impedance matching of the antenna to the transceiver/transmission line is often required, although exceptions exist, e.g., in [28] a co-design approach canceled the need for a matching network by optimizing the antenna and IC for conjugate matching. However, when present, matching networks still occupy valuable WiNoC transceiver area.
5. antenna efficiencies may be very low (part of this may be attributable to impedance mismatching), which means that additional transmission power is required compared to the impedance-matched case.
6. reported results for transmission gain obscure the specification of antenna gain itself, making antennas used within such transmission gain results not "portable" to other physical settings.
7. reported bandwidths are in many cases larger than our minimum estimated bandwidth of 10 GHz, which is promising.

Given the novelty of the WiNoC environment, for WiNoC antennas, we may need to deviate from conventional antenna theory meant for 3D far-field communication since the actual WiNoC antenna requirements differ substantially from those used in conventional designs. The challenges in WiNoC antennas also provide unique opportunities to design novel on-chip antennas using innovations in nanotechnology and nanomaterials. What follows is a non-exhaustive list of ideas that we have found in the literature for novel compact antenna designs:

- *Inductive Coupling* commonly used for power transmission over short distances, laterally and vertically coupled inductances may be used to communicate between the closest transceivers [29].
- *Metamaterials* as also suggested by Singh [13], metamaterials designed for mm wave operation can be used to isolate and focus radiation, especially in the higher bands of interest. They may also be used to reduce the antenna size, especially at the higher end of the frequency range, i.e., the THz regime.
- *Pulse-Driven Antennas* although only demonstrated for HF transmission [30] thus far, the idea of actual pulses driving antennas without impedance matching is a very promising and intriguing possibility for WiNoCs, as it can further reduce area/power requirements and minimize circuitry required for modulation.
- *Plasmonic Antennas* plasmonics, another by-product of nanophotonics and nanomaterials, provide novel radiation mechanisms to enable electromagnetic radiation using plasmon coupled waves on metal nanostructures. A recent paper on this idea [30] claims that the concept can be extended to THz radiation, and this would be a very promising way to build compact antennas with moderate gain.
- *Bonding-Wire Antennas* another unique possibility for WiNoCs is the use of existing bond wires at the perimeter of the chip as antennas for on-chip communication (e.g., [31]). While this would require unique optimizations to the geometry of the wires and an infrastructure to (de)-couple radiation, it is possible that some of the (dummy) IC bond-wires could be reserved for this purpose.
- *MEMS/3D Structures* over the last 20 years, the MEMS community has amassed many CMOS compatible fabrication options to build folding/assembling 3D (strictly speaking 2.5D) metal structures that can reach 100s of microns in length [32]. It may be possible to borrow ideas to build folded or vertical antenna structures that can liberate area constraints substantially.

- *2D Reflectors/Directors* on-chip antennas can benefit from planar and/or vertically stacked reflector/director metal structures (once again built using largely MEMS technology) to improve the antenna directivity and efficiency. Actually, this would be easier to implement for planar structures than fully 3D cases in conventional large antennas.

4 Example Antenna Designs and Resulting Wireless Channels

Here we first comment on two of the most promising designs from the literature. For our work in [2], we considered separate antennas for Tx and Rx, specifically four Tx antennas and four Rx antennas at each router, placed on a layer *above* the router substrate. These antennas were required to cover only a part (approximately ¼ of) the 80 GHz band from 50 to 130 GHz. This design was a scaling of that found in [13]. In that reference, the author employed a metamaterial—essentially an array of regularly-distributed holes in the substrate—to improve the gain and radiation efficiency of a patch in the frequency range of approximately 600–950 GHz. The author reported gains of $\sim$8 dB, and bandwidth $\sim$30%. By scaling dimensions by approximately a factor of 10 to the mm-wave band we assume similar performance. The area of these antennas is large enough such that they must be placed on a layer above the routers (with vertical feeds). We assume inefficiencies in scaling, and allowing for fabrication imperfections and implementation losses, in our link budgets described in [2] we have decreased the gain from 8 dB to a value of 0 dB.

An alternative design for the 60 GHz range appears in [12], where both inverted-F and meander dipole antennas were investigated. These designs attain (measured) gains from approximately -2 to -9 dB, without any enhancement from metamaterials (which include suppression of surface waves, fringing fields, etc.).

For our new example here, we have conducted full-wave simulations in HFSS for some example WiNoC antenna designs, and have gathered results on the antennas themselves, as well as on the resulting wireless channels the communication signals must traverse. Again, in the interest of brevity, we do not discuss WiNoC channel characteristics in detail—see Sect. 2.3 and [7]. Here we describe the design, and discuss its performance in terms of impedance match, overall channel path loss (which incorporates antenna gains[2]), and wireless channel dispersion, which can limit usable bandwidth. The design employs a center frequency of 150 GHz, and we consider performance over a total frequency span of 40 GHz. The design that we consider consists of upright quarter-wavelength monopoles and half-wavelength printed dipoles. The design is enclosed in a ceramic casing. A depiction of the design is shown in Fig. 2.

The design is for a chip of size 20 mm by 20 mm, with five monopole antennas—one at each corner and one in the center—in addition to the three printed dipole antennas. Dimensions are in Fig. 2. The dielectric slab atop the ground plane is polyimide with relative dielectric constant $\varepsilon_r = 4$. We have used a ceramic casing for thermal reasons, and also because a metal casing would induce stronger and more reflections, causing more severe multipath distortion (worth noting is that use of plastic casing changed results only slightly from that of the ceramic case). For these designs, the impedance matching is quantified by the scattering parameter S_{ii}, for $i = 1, 2, 3, 4, 5, 1H, 2H, 3H$, with the "H"

[2] Note that this is hence identical to "transmission gain," but the term path loss is prevalent in the communications literature.

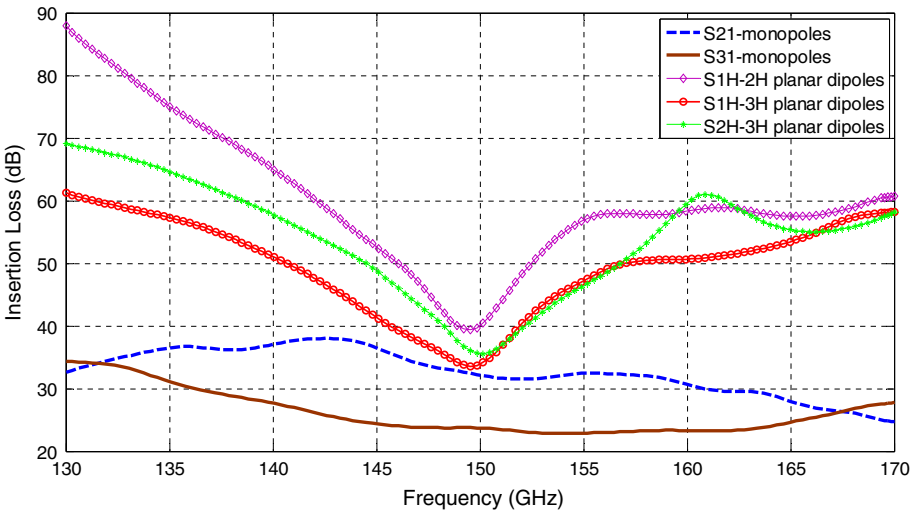

Fig. 3 Insertion losses for various antenna pairs in the design of Fig. 2

denoting horizontal polarization of the three dipoles. The S_{ii} values are lower than -10 dB for the frequency range of 149–151 and 130–162 GHz for the planar dipoles and monopoles, respectively.

We show in Fig. 3 the channel attenuation versus frequency for the two types of antennas in the design. Here the side-to-side monopole channel results are denoted S_{21}, whereas the diagonal monopole channel results are denoted S_{31}. If we define bandwidth as the range of frequencies where the insertion loss variation $\Delta|S_{i1}| < 2$ dB[3] for $i = 2, 3$, we can observe that for the 1H–2H dipole link, the 2H–3H dipole link, and the 1H–3H dipole link, the maximum single-channel bandwidths available are approximately 15 GHz (155–170 GHz), 5 GHz (165–170 GHz), and 6 GHz (157–163 GHz), respectively. For the monopoles, the maximum side-to-side single channel-bandwidth is 10 GHz (150–160 GHz). For the monopole diagonal channels, the maximum available single-channel bandwidth is 20 GHz (145–165 GHz). Excepting the monopole channels, approximately 3 channels of bandwidth on the order of 3 GHz are available for use from the dipoles-only network in a frequency division arrangement. However, the dipole channels exhibit a *much* higher insertion loss than the monopole channels, due to the proximity to the ground plane. Although etching out an area of the ground plane beneath the monopoles would improve their performance, this would come at the cost of radiation leakage below, where the active devices lay. It is also important to note that in order to use the dipole and monopole channels simultaneously, sufficient isolation and filtering is needed so that the channels do not interfere with each other.

The obvious frequency selectivity of the channels illustrated in Fig. 3 has led us to evaluate remedial measures, specifically equalization. Equalizers for wired transmissions on long microstrip or striplines on circuit boards can currently run at 10–25 Gb/s [33, 34], and these often consist of transmitter pre-filters as well as decision feedback equalizers (DFEs) at the receiver. Equalizer lengths (# filter coefficients) are presently at least 16 [33].

[3] The 2 dB value is arbitrary, and could be adjusted. Consequences of the non-flat channel amplitude response could be required equalization, which we discuss subsequently.

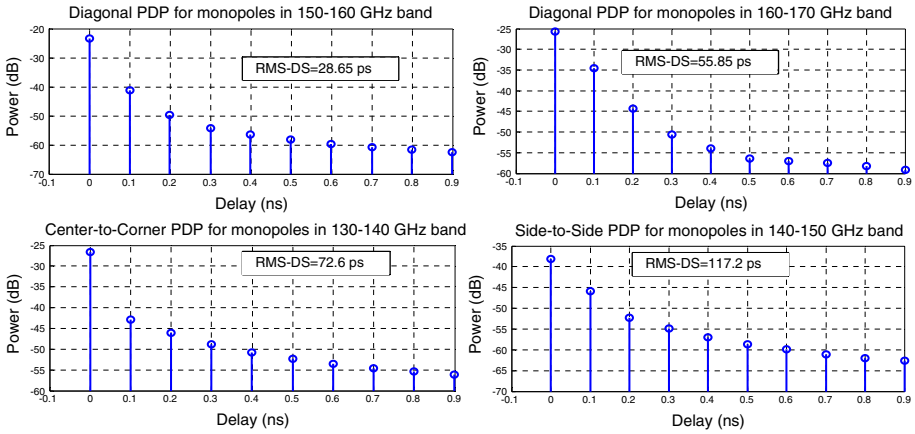

Fig. 4 Unequalized power delay profiles of monopoles channels in different frequency bands

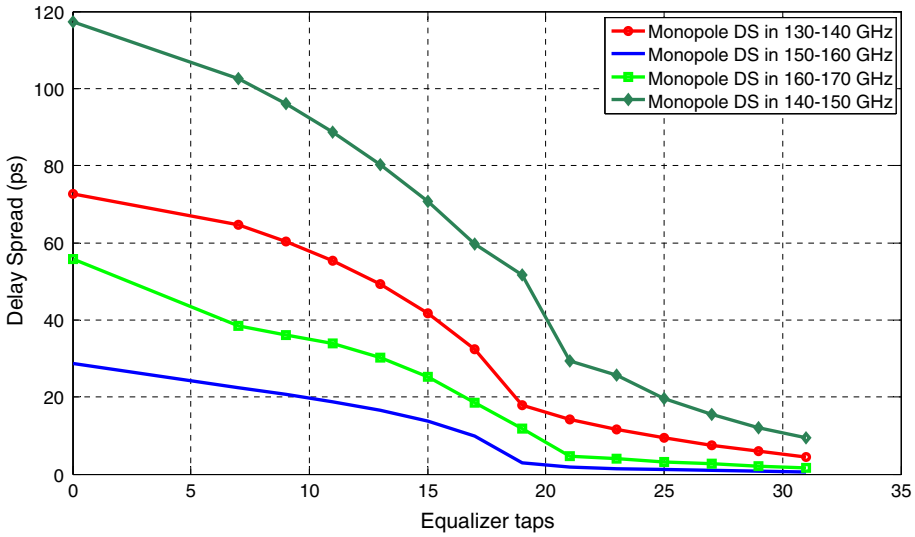

Fig. 5 RMS delay spread versus number of linear (zero-forcing) equalizer taps for channels in Fig. 4

Here we briefly illustrate performance enhancements attainable with simple zero-forcing (ZF) equalizers [35] and DFEs. We use the time domain impulse response (inverse Fourier transform of the S_{i1} parameters) for this evaluation.

Figure 4 shows the unequalized (original) channel impulse responses in terms of power delay profiles for the side, diagonal, and center-to-corner channels in different frequency bands of the design. The measure of dispersion we use is the root-mean square delay spread (RMS-DS) [35], the reciprocal of which is a rough measure of usable bandwidth. From this figure, the worst (largest) RMS-DS pertains to the side-to-side monopole channel between 140 and 150 GHz.

To investigate the improvement that equalization has on the channel impulse responses of both designs, linear ZF and DF equalizers were designed and applied to the channel

responses in Fig. 4. Figure 5 shows the resulting RMS-DS versus equalizer length for the four channels with ZF equalization. One estimate for a channel's coherence bandwidth is the reciprocal of five times the RMS-DS [35]; using this, if we desire an equalized bandwidth of 10 GHz, this requires an equalized RMS-DS equal to 20 ps. Equalizer lengths of 9, 17, 19, and 25 coefficients can attain this for the channels shown in Fig. 4 whereas only 2 feedforward and 2 feedback taps are enough with the more effective DFE. To attain an RMS-DS of 2 ps for the channel with the largest RMS-DS of Fig. 4, 8 feedforward and 4 feedback taps are needed with the DFE whereas 41 taps are required with the zero-forcing equalizer, illustrating the potential for very low dispersion with the DFE.

5 Conclusion

In this paper we described antennas and corresponding wireless channels for wireless networks on chips. After providing a summary of the antenna design problem that included basic characteristics such as gain, impedance match, and bandwidth, we also commented on structural and multiple access considerations, and basic WiNoC channel characteristics. This was followed by a review of the literature on antennas, in which we found that nearly all prior designs limit themselves to planar (printed structures), and most results (all but three) were limited to a maximum frequency of 30 GHz—far too low to enable the tens of Gbps data rates that WiNoCs will require. A summary of the existing designs led us to propose consideration of multiple completely novel approaches. We then presented our example designs for a 40 GHz band centered at 150 GHz and found that quarter-wave monopoles may offer a promising alternative to the conventional printed antenna approach, as channel losses and bandwidths are superior to those of printed antennas. In specific small frequency bands where the printed dipole insertion loss is small enough, they can be used to augment system capacity. Multipath propagation will prove the limiting factor for WiNoC data rates: we showed that simple linear or decision feedback equalizers could reduce dispersion to enable several channels of bandwidth approximately 10 GHz in our 40 GHz wide band. It is clear from our review and example designs that antenna design and wireless channel characterization for WiNoCs is a rich subject for future research.

Acknowledgements The authors would like to thank ANSYS, Inc., for the generous use of the HFSS® software. This research was supported by the NSF Award ECCS-1129010.

References

1. Borkar, S. (2007). Thousand core chips: A technology perspective. In *Proceedings of 44th design automation conference,* San Diego, CA, 4–8 June 2007.
2. Matolak, D. W., Kodi, A., Kaya, S., DiTomaso, D., Laha, S., & Rayess, W. (2012). Wireless networks-on-chips: Architecture, wireless channel, and devices. *IEEE Wireless Communications Magazine, 19*(5), 58–65.
3. Kaya, S., Laha, S., Kodi, A., Ditomaso, D., Matolak, D. W., & Rayess, W. (2013). On ultra-short wireless interconnects for NoCs and SoCs: Bridging the 'THz Gap'. In *IEEE international midwest symposium on circuits and systems*, Columbus, OH, 4–7 August 2013.
4. Ditomaso, D., Kodi, A., Kaya, S., Laha, S., Matolak, D. W., & Rayess, W. (2013). Energy-efficient adaptive wireless NoCs architecture. In *NOCS 2013*, Tempe, AZ, 21–24 April 2013.

5. Ganguly, A., Chang, K., Deb, S., Pande, P. P., Belzer, B., & Teuscher, C. (2011). Scalable hybrid wireless network-on-chip architectures for multicore systems. *IEEE Transactions on Computers, 60*(10), 1485–1502.
6. Lee, S., Tam, S., Pefkianakis, I., Lu, S., Chang, M. F., Guo, C., et al. (2009). A scalable micro wireless interconnect structure for CMPs. In *Proceedings of MobiCom'09*, Beijing, China, 20–25 September 2009.
7. Matolak, D. W., Kodi, A., & Kaya, S. (2013). Channel modeling for wireless networks-on-chips. *IEEE Communications Magazine, 51*(6), 180–186.
8. Wang, Y., Makadia, D., & Margala, M. (2006). On-chip integrated antennas—the first challenge for reliable on-chip wireless interconnects. In *Canadian conference on electrical and computer engineering* (pp. 2322–2325), Ottawa, Canada 7–10 May 2006.
9. He, X., Li, J., Zhang, M., & Qi, S. (2010). Improvement of integrated dipole antenna performance using diamond for intra-chip wireless interconnection. In *IEEE International Conference IC Design and Technology* (pp. 248–251), Grenoble, France, 2–4 June 2010.
10. Moriyama, W., Kubota, S., Kimoto, K., Sasaki, N., & Kikkawa T. (2008). On-chip micro-meander-antennas for silicon LSI wireless interconnects. In *IEEE international symposium antennas and propagation* (pp. 1–4), 5–11 July 2008.
11. Kim, K., & Ko, K. (1999). Integrated dipole antennas on silicon substrates for intra-chip communication. *IEEE Antennas and Propagation Society International Symposium, 3,* 1582–1585.
12. Titz, D., Ben Abdeljelil, F., Jan, S., Ferrero, F., Luxey, C., Brachat, P., et al. (2012). Design and characterization of CMOS on-chip antennas for 60 GHz communications. *Radioengineering, 21*(1), 324–332.
13. Singh, G. (2010). Design considerations for rectangular microstrip patch antenna on electromagnetic crystal substrate at terahertz frequency. *Infrared Physics and Technology, 53*(1), 17–22.
14. Uzunkol, M., Gurbuz, O. D., Golcuk, F., & Rebeiz, G. M. (2013). A 0.32 THz SiGe 4 x 4 imaging array using high-efficiency on-chip antennas. *IEEE Journal of Solid-State Circuits, 48*(9), 2056–2066.
15. Golcuk, F., Gurbuz, O. D., & Rebeiz, G. M. (2013). A 0.39–0.44 THz 2 x 4 amplifier-quadrupler array with peak EIRP of 3–4 dBm. *IEEE Transactions on Microwave Theory and Techniques, 61*(12), 4483–4491.
16. Ojefors, E., Pfeiffer, U. R., Lisauskas, A., & Roskos, H. G. (2009). A 0.65 THz focal-plane array in a quarter-micron CMOS process technology. *IEEE Journal on Solid-State Circuits, 44*(7), 1968–1976.
17. Tavakoli, E., Tabandeh, M., & Kaffash, S. (2011). An optimized phased-array antenna for intra-chip communications. In *Loughborough antennas and propagation conference* (pp. 1–4), Loughborough, UK, 14–15 November 2011.
18. Deb, S., Ganguly, A., Chang, K., Pande, P., Belzer, B., & Heo, D. (2010). Enhancing performance of network-on-chip architectures with millimeter-wave wireless interconnects. In *Proceedings of IEEE international conference application-specific systems, architectures and processors* (ASAP 2010) (pp. 73–80), 7–9 July 2010.
19. Pan, S., Wang, D., & Capolino, F. (2011). Novel high efficiency CMOS on-chip antenna structures at millimeter waves. In *IEEE international symposium on antennas and propagation* (pp. 907, 910), 3–8 July 2011.
20. Marnat, L., Carreno, A. A. A., Conchouso, D., Martinez, M. G., Foulds, I. G., & Shamim, A. (2013). New movable plate for efficient millimeter wave vertical on-chip antenna. *IEEE Transactions on Antennas and Propagation, 61*(4), 1608–1615.
21. Kubota, S., Kimoto, K., Sasaki, N., Toya, A., & Kikkawa, T. (2011). A novel 10 Gb/s silicon on-chip UWB twiggy antenna for intra-package communication. In *IEEE international symposium antennas and propagation* (pp. 82–85), 3–8 July 2011.
22. Yeh, H., Melde, K., & Eisenstadt, W. (2012). Design and packaging of small 60 GHz antenna array for multi-chip communication. In *Proceedings of IEEE international conference wireless information technology and systems (ICWITS),* Maui, HI, 11–16 November 2012.
23. Melde, K., Yoo, S., & Yeh, H. (2015). On-chip antenna arrays for multi-chip RF data transmission. In *European conference on antennas and propagation* (pp. 1–4), 13–17 April 2015.
24. Kikkawa, T., Kimoto, K., & Kubota, S. (2010). Analysis of silicon on-chip integrated antennas for intra- and inter-chip wireless interconnects. In *European solid-state device research conference* (pp. 114–117), Seville, Spain, 14–16 September 2010.
25. Yordanov, H., & Russer, P. (2010). Area-efficient integrated antennas for inter-chip communication. In *European Microwave Conference* (pp. 401–404), Paris, France, 28–30 September 2010.
26. Wu-Hsin, C., Sanghoon, J., Sayilir, S., Willmot, R., Tae-Young, C., Dowon, K., et al. (2009). A 6-Gb/s wireless inter-chip data link using 43-GHz transceivers and bond-wire antennas. *IEEE Journal of Solid-State Circuits, 44*(10), 2711–2721.

27. Lin, J., et al. (2007). Communication using antennas fabricated in silicon integrated circuits. *IEEE Journal of Solid-State Circuits, 42*(8), 1678–1687.
28. Cheema, H. M., & Shamim, A. (2013). The last barrier: On-chip antennas. *IEEE Microwave Magazine, 14*(1), 79–91.
29. Radecki, A., Yuxiang, Y., Miura, N., Aikawa, I., Take, Y., Ishikuro, H., et al. (2012). Simultaneous 6-Gb/s data and 10-mW power transmission using nested clover coils for noncontact memory card. *IEEE Journal Solid-State Circuits, 47*(10), 2484–2495.
30. Keller, S. D., Palmer, W. D., & Joines, W. T. (2010). Digitally driven antenna for HF transmission. *IEEE Transactions on Microwave Theory and Techniques, 58*(9), 2362–2367.
31. Davoyan, A. R., Maksymov, I. S., & Kivshar, Y. S. (2011). Tapered plasmonic Yagi-Uda nanoantennas for emission enhancement and broadband communication. In *International quantum electronics conference* IQEC/CLEO Pacific Rim 2011 (pp. 646–648), Sydney, Australia, 28 August–1 September 2011.
32. Nenzi, P., Tripaldi, F., Varlamava, V., Palma, F., & Balucani, M. (2012). On-chip THz 3D antennas. In *2012 IEEE 62nd electronic components and technology conference (ECTC)* (pp. 102–108), 29 May–1 June 1 2012.
33. Cain, J. (2013). Vice President, Platform Engineering Group, Cisco Systems, private communication, University of South Carolina Department of Electrical Engineering Seminar, 25 November 2013.
34. Cideciyan, R. D., Gustlin, M., Li, M. P., Wang, J., & Qant, Z. (2013). Next generation backplane and copper cable challenges. *IEEE Communications Magazine, 51*(12), 130–136.
35. Proakis, J. G., & Salehi, M. (2007). *Digital communications* (5th ed.). New York, NY: McGraw-Hill.

William Rayess received the B.E. degree in computer and communications engineering from Notre Dame University in Lebanon in 2008, the MCTP degree from Ohio University in 2009, and started working toward the Ph.D. degree in Electrical Engineering at the Russ College of Engineering, Ohio University in 2011 and received his Ph.D. at the University of South Carolina in December 2016. He is a student member of the IEEE.

David W. Matolak received the B.S. degree from Pennsylvania State University, University Park, the M.S. degree from the University of Massachusetts, Amherst, MA, and the Ph.D. degree from the University of Virginia, Charlottesville, all in electrical engineering. He has worked for more than 20 years on communication systems, with the Rural Electrification Administration, Washington, DC, the UMass LAMMDA Laboratory, Amherhst, AT&T Bell Laboratories, North Andover, MA, the University of Virginias Communication Systems Laboratory, Lockheed Martin Tactical Communication Systems, Salt Lake City, UT, the MITRE Corporation, McLean, VA, and Lock-heed Martin Global Telecommunications, Reston, VA. From 1999 to August 2012, he was with the School of Electrical Engineering and Computer Science at Ohio University, and since August 2012, he has been with the Department of Electrical Engineering at the University of South Carolina. He is a senior member of the IEEE.

Savas Kaya received the Ph.D. degree from Imperial College of Science, Technology and Medicine, London, in 1998, for his work on strained Si quantum wells on vicinal substrates, following the MPhil degree in 1994 from the University of Cambridge. He was a post-doctoral researcher at the University of Glasgow between 1998 and 2001, carrying out research in transport and scaling in Si/SiGe MOSFETs, and fluctuation phenomena in decanano MOSFETs. He is currently with the Russ College of Engineering at Ohio University, Athens. His other interests include transport theory, device modeling and process integration, nanofabrication, nanostructures and nanosensors. He is a senior member of the IEEE.

Avinash Karanth Kodi received the M.S. and Ph.D. degrees in Electrical and Computer Engineering from the University of Arizona, Tucson, in 2003 and 2006, respectively. He is currently an associate professor of Electrical Engineering and Computer Science at Ohio University, Athens. He received the National Science Foundation (NSF) CAREER Award in 2011. His research interests include computer architecture, optical interconnects, chip multiprocessors (CMPs) and network-on-chips (NoCs). He is a senior member of the IEEE.